The American Journal of Pathology, Vol. 185, No. 5, May 2015

The American Journal of
PATHOLOGY
ajp.amjpathol.org

See related Commentary on page 1198

CARDIOVASCULAR, PULMONARY, AND RENAL PATHOLOGY

Protective Role of Insulin-Like Growth Factor-1 Receptor in Endothelial Cells against Unilateral Ureteral Obstruction—Induced Renal Fibrosis

Ming Liang,*† Lauren E. Woodard,‡ Anlin Liang,† Jinlong Luo,† Matthew H. Wilson,‡ William E. Mitch,† and Jizhong Cheng†

From the Department of Nephrology, Guangzhou First People's Hospital, Guangzhou Medical University, Guangzhou, China; the Nephrology Division,† Department of Medicine, Baylor College of Medicine, Houston, Texas; and the Division of Nephrology and Hypertension,‡ Department of Medicine, Vanderbilt University, and Department of Veterans Affairs, Nashville, Tennessee*

Accepted for publication January 15, 2015.

Address correspondence to Jizhong Cheng, M.D., Nephrology Division, Department of Medicine, Baylor College of Medicine, One Baylor Plaza, Houston, TX 77030. E-mail: jizhongc@bcm.edu.

Insulin-like growth factor-1 receptor (IGF-1R) can regulate vascular homeostasis and endothelial function. We studied the role of IGF-1R in oxidative stress—induced endothelial dysfunction. Unilateral ureteral obstruction (UUO) was performed in wild-type (WT) mice and mice with endothelial cell (EC)—specific IGF-1R knockout (KO). After UUO in endothelial IGF-1R KO mice, endothelial barrier dysfunction was more severe than in WT mice, as seen by increased inflammatory cell infiltration and vascular endothelial (VE)—cadherin phosphorylation. UUO in endothelial IGF-1R KO mice increased interstitial fibroblast accumulation and enhanced extracellular protein deposition as compared with the WT mice. Endothelial barrier function measured by transendothelial migration in response to hydrogen peroxide (H_2O_2) was impaired in ECs. Silencing IGF-1R enhanced the influence of H_2O_2 in disrupting the VE—protein tyrosine phosphatase/VE-cadherin interaction. Overexpression of IGF-1R suppressed H_2O_2-induced endothelial barrier dysfunction. Furthermore, by using the *piggyBac* transposon system, we expressed IGF-1R in VE cells in mice. The expression of IGF-1R in ECs also suppressed the inflammatory cell infiltration and renal fibrosis induced by UUO. IGF-1R KO in the VE-cadherin lineage of bone marrow cells had no significant effect on the UUO-induced fibrosis, as compared with control mice. Our results indicate that IGF-1R in the endothelium maintains the endothelial barrier function by stabilization of the VE—protein tyrosine phosphatase/VE-cadherin complex. Decreased expression of IGF-1R impairs endothelial function and increases the fibrosis of kidney disease. *(Am J Pathol 2015, 185: 1234—1250; http://dx.doi.org/10.1016/j.ajpath.2015.01.027)*

Chronic kidney disease (CKD) is a major health care problem that ultimately progresses to renal failure and the need for dialysis and/or renal transplantation.[1] Exaggerated inflammation plays a critical role in acute and chronic renal diseases, including obstructive kidney disease, glomerulonephritis, and ischemia-reperfusion—induced nephropathy. Although systemic endothelial dysfunction is associated with pathological changes in CKD, the role of the renal endothelium in the initiation and the progression of renal inflammation and fibrosis remains largely elusive. In addition to its classic barrier function, the endothelium is a key player in physiological processes, such as the regulation of tissue inflammation and of thrombosis.[2,3] Although endothelial barrier integrity is essential to prevent inflammatory responses, few studies have explored the potential contribution of impaired endothelial barrier function to CKD-induced nephropathy, including fibrosis.[4]

The insulin-like growth factor-1 receptor (IGF-1R) is a member of the tyrosine kinase receptor superfamily that is involved in the regulation of cellular proliferation, differentiation, and survival.[5] IGF-1R contributes to the maintenance of paracellular barrier function in salivary gland cells

Supported by NIH grants RO1-DK095867 and R37-DK37175, VA grant 1I01 BX002190, American Heart Association grant 10SDG2780009, Science and Technology Planning Project of Guangzhou, China, grant 2012J4300081, and a Dr. and Mrs. Harold Selzman grant.

Disclosures: None declared.

http://dx.doi.org/10.1016/j.ajpath.2015.01.027

via the expression and distribution of tight junction proteins.[6] There are an increasing number of studies that show that IGF-1R is a protective factor in endothelial cells (ECs).[7] IGF-1 signaling inhibits hydrogen peroxide (H_2O_2)–induced apoptosis in human umbilical vein ECs (HUVECs) by reducing mitochondrial dysfunction. Specifically, the protective mechanism of IGF-1 involves preserving the mitochondrial membrane potential and reducing caspase-3 activity. Specific binding of IGF-1 to IGF-1R has been demonstrated in kidney and retinal ECs,[8–10] but whether IGF-1R plays a protective role in CKD-induced pathological responses is unknown.

The vascular endothelium sits at the interface between the blood stream and the vessel wall and is involved in the regulation of metabolic hemostatic and immunological processes. The regulation of EC contacts is of central importance for the barrier function of the blood vessel wall and for the control of leukocyte extravasation. Despite the participation of several adhesion molecules and receptors in the control of endothelial barrier, most of the currently known mechanisms involve vascular endothelial–cadherin (VE-cadherin), an essential adhesion molecule for the stability of endothelial junctions. VE-cadherin is believed to be of dominant importance for the stability of EC contacts and, consequently, most mechanisms that affect the stability of endothelial junctions target VE-cadherin. The factors histamine, thrombin, tumor necrosis factor (TNF)-α, vascular endothelial growth factor (VEGF)-A, and oxidative stress were shown to increase tyrosine phosphorylation of various components of the cadherin-catenin complex and increase permeability of cultured EC monolayers.[11]

On the basis of these previous findings,[7–10] we hypothesized that IGF-1R has a critical role in the maintenance of capillary architecture and function during CKD. Because IGF-1 acts as an important survival factor for multiple cell types, we undertook this study to investigate whether IGF-1R favorably affects the barrier function of vascular ECs.

Materials and Methods

Animals

To generate mice with IGF-1R knocked out in the endothelium, mice carrying a floxed IGF-1R allele[12] were bred with VE-cadherin-Cre mice (Jackson Laboratory, Bar Harbor, ME), in which Cre is only expressed in ECs. After backcrossing, the IGF-1R$^{f/f}$/VE-cadherin-Cre^{+} [IGF-1R knockout (KO)] mice were obtained. Although whole body KO of IGF-1R is fatal and leads to embryonic death,[13] we found that KO of IGF-1R in ECs did not cause abnormality in gross appearance or male/female ratio. Mice carrying this EC-specific mutation were of normal size and weight and did not display any apparent renal pathology in our experimental period. Red fluorescent protein (RFP)^{flox}–green fluorescent protein (GFP) mice [B6.Cg-Tg(CAG-DsRed-EGFP)5Gae/J, stock number 008705][14] were bred with VE-cadherin-Cre mice to evaluate the VE-cadherin-Cre efficiency. Mice were housed in a conventional animal facility with a 12-hour light/dark cycle. Genotyping was performed using tail DNA. IGF-1R KO and wild-type (WT) littermate control (VE-cadherin-Cre–negative) male mice, aged 3 to 4 months, were used in experiments. All animal experiments were conducted in accordance with accepted animal protocols (AN-6188 and D1557) approved by the Institutional Animal Care and Use Committee at the Baylor College of Medicine (Houston, TX).

Plasmid and Adenovirus Preparation

The adenovirus expressing *IGF-1R* was constructed by inserting the *IGF-1R* cDNA into the pTracker-CMV vector, and the adenovirus was prepared as reported previously.[12] We constructed the plasmid pT-VE-cad-IGF-1R, a transposon containing the cDNA of IGF-1R under control of the VE-cadherin promoter, by InFusion cloning (Clontech, Mountain View, CA). pT-VE-cad-IGF-1R has the same ampicillin-resistant backbone, *piggyBac* transposon inverted repeats, and polyA signal components as the previously published transposon plasmids pT-tight-Luc[15] and pT-tight-GSTA4.[16] The VE-cadherin promoter was cloned by RT-PCR from mouse genomic DNA. We generated the construct by gel purification of the linear plasmid backbone fragment containing the *piggyBac* inverted repeats. We PCR amplified both the VE-cadherin promoter and the IGF-1R cDNAs with the following primers: VE-cad_F1 (5′-AGATACTCGAGCTAGCCTAGTAGCAGAAACAAGGTC-3′) and VE-cad_R1 (5′-GGAGCCAGACTTCATGGTGGCGGCAGTCTGTCCAGGGCCGAG-3′); or IGF-1R_F1 (5′-ATGAAGTCTGGCTCCGGA-3′) and IGF-1R_R1 (5′-TCGACAAGCTTATCGATTCAGCAGGTCGAAGACTG-3′). The primers generated regions of 15-bp homology, as required by the InFusion enzyme. The primers also introduced a Kozak sequence and two restriction enzyme sites: a NotI site between the VE-cadherin promoter and the IGF-1R genes and a MluI site between the IGF-1R sequence and the polyA signal. The three fragments (VE-cadherin promoter, IGF-1R cDNA, and backbone) were joined using InFusion, following the manufacturer's instructions.

Reagents and Antibodies

Penicillin, streptomycin, Dulbecco's modified Eagle's medium, and fetal bovine serum were obtained from Invitrogen Life Technologies (Carlsbad, CA). The protein assay kit was from Bio-Rad (Hercules, CA). The monoclonal α-smooth muscle actin (SMA)–fluorescein isothiocyanate (FITC) antibody, dextran-FITC, and Evans Blue Dye were from Sigma-Aldrich (St. Louis, MO); VE-cadherin and CD31 antibodies were from BD Biosciences (San Jose, CA); IGF-1Rβ, von Willebrand factor, and platelet-derived growth factor receptor (PDGFR)-β antibodies were from Santa Cruz Biotechnology (Santa Cruz, CA); phosphorylated VE-cadherin, F-actin–phalloidin–FITC, fluorescent secondary

antibodies, and Tyramide Signal Amplification Kit were from Invitrogen (Carlsbad, CA); protein tyrosine phosphatase (PTP) receptor β (VE-PTP) antibody was from Gene Tex (Irvine, CA); CD42 and CD144 (VE-cadherin) antibodies were from eBioscience (San Diego, CA); antibody against PDGFR-α was from R&D (Minneapolis, MN); antibodies against GFP (rabbit) were from Abcam (Cambridge, MA); DAPI was from Southern Biotech (Birmingham, AL); and macrophage marker F4/80 and rabbit anti−α-SMA antibodies were from Abcam (Cambridge, MA).

Renal Interstitial Fibrosis Model

Unilateral ureteral obstruction (UUO) or sham surgery was performed on 3- to 4-month-old male mice, as described previously.[17,18] Male mice were anesthetized with an i.p. of xylazine and ketamine cocktail (8.8 mg/kg xylazine and 130 mg/kg ketamine). Kidney tissue was harvested 3 or 7 days after UUO or sham surgery. Because previous studies showed no differences between these time points in sham−operated on mice,[17] a single time point (day 3 or 7) was used for sham controls in each experiment. Under anesthesia, the left ureter was isolated and ligated for 3 or 7 days. For *in vivo* gene delivery of *IGF-1R* in renal ECs, the plasmids pCMV-*piggyBac*, pT-TetOn, and pT-*VE-cad-IGF-1R* were mixed with endotoxin-free hydrodynamic injection solution QR (Mirus, Madison, WI) and injected into the renal vein of one kidney. Subsequently, UUO was generated. After 7 days, animals were sacrificed and the kidneys were analyzed.

Renal IRI

We used an established mouse model of kidney ischemia/reperfusion injury (IRI) induced by clamping of bilateral renal pedicles. Male mice (age, 3 to 4 months; weight, 20 to 25 g) were anesthetized with an i.p. injection of 2 mL/kg combination anesthetic. After abdominal incision, left and right renal pedicles are bluntly dissected, and bilateral ischemia was induced by clamping of the renal pedicle for 30 minutes using a small microvascular clamp (Roboz Surgical Instruments, Gaithersburg, MD), stopping blood flow. During the procedure, animals were kept on a heating pad and hydrated with warm saline. After 30 minutes of ischemia, the clamps were removed, allowing reperfusion. The wounds were sutured, and the animals were allowed to recover. Sham-treated mice had identical surgical procedures except for clamping of the kidneys. Mice were euthanized at 72 hours and 1 week after reperfusion, and kidneys were harvested for Western blot analysis.

BM Isolation and Transplantation

Bone marrow cells (BMCs) were obtained from tibias and femurs of WT or IGF-1R KO mice. The transplant was generated by injecting 5×10^6 BMCs into the lateral tail vein of lethally irradiated (11 Gy) WT mouse recipients.[19] Mice received kanamycin in their drinking water (2 mg/mL) for 14 days after transplantation. Mice were divided into two groups with six animals in each group: WT mice were transplanted with BMCs isolated from WT (control) or from VE-cadherin-Cre^+/IGF-$1R^{f/f}$ mice. UUO surgeries were performed 2 months later. After 7 days, the animals were euthanized under anesthesia and the kidneys were removed for analysis.

Assessment of Renal Function

Blood samples were collected for creatinine measurement after sham surgery or day 7 after UUO. Serum creatinine was measured using the Quanti Chrom Creatinine Assay Kit (Jaffe method) as per the manufacturer's instructions (Sigma-Aldrich).

Histology and Immunohistochemistry

For histological analysis, the kidneys were prepared by perfusion of the mice through the left ventricle and slides of the kidney were prepared as described.[18] Histology scoring was performed by examining periodic acid−Schiff−stained kidney sections of five mice in each group by an experienced pathologist (M.L.) on coded slides. Immunohistochemical staining was performed on kidney tissues using procedures established in our laboratory.[17,18] For double-immunofluorescence staining, after primary antibodies, fluorescent secondary antibodies were incubated. DAPI was used to stain the nuclear DNA. The Nikon Eclipse 80i fluorescence microscope (Nikon, Melville, NY) was used to capture the images, and the negative control was either an isotype-matched IgG or phosphate-buffered saline with Tween. The areas of positive signal were measured using the NIS-Elements BR 3.0 program (Nikon). Picro-Sirius Red staining was performed for assessment of collagen deposition, as described.[18] The amount of cortical fibrillary collagen was determined by observing areas stained with Picro-Sirius Red with a Nikon Eclipse 80i fluorescence microscope. To determine GFP expression in RFP^{flox}-GFP/VE-cadherin-Cre^+ mice, the cryotissue sections were stained with anti-GFP primary antibody. After washing three times, the samples were stained with anti-rabbit IgG antibody conjugated to Alexa Fluor Cy5 dye (BD Biosciences). The images were obtained using a Zeiss LSM-510 inverted deconvolution microscope with a Zeiss Plan Apochromat 63 (numerical aperture, 1.4) objective lens (Nikon).

Images (×400 magnification) from each section were analyzed in a blinded manner (J.L.) and quantified using Image-Pro Plus software version 4.5 (Media Cybernetics, Silver Spring, MD). The results were expressed as the percentage of total tubulointerstitial area stained.

H_2O_2 Measurements

Kidneys were harvested and homogenized in 250 μL sucrose buffer on ice, followed by protein quantitation (Bradford method). H_2O_2 was measured as described previously.[20] The method takes advantage of the conversion of Fe^{2+} to Fe^{3+} in

the presence of H_2O_2, followed by detection of Fe^{3+}-xylenol orange complex. Briefly, kidney lysate (100 μg/20 μL) was added to 180 μL assay buffer, followed by measurement of absorbance at 560 nm. Absorbance values were normalized to the absorbance of wells containing assay buffer alone and expressed as OD.

Measurement of mRNA Expression

Total kidney RNA was isolated by the RNeasy kit (Qiagen, Valencia, CA). Real-time RT-PCR was performed with the Opticon real-time RT-PCR machine (MJ Research, Waltham, MA). The primers used were mouse fibronectin (forward, 5′-TTCCAGAAGGTGATGAG-3′; and reverse, 5′-TCATGGCAATGCAGGACAGGAAGA-3′), collagen I (forward, 5′-TTCCAGAAGGTGATGAG-3′; and reverse, 5′-TCATGGCAATGCAGGACAGGAAGA-3′), IGF-1R (forward, 5′-CGGCCAAGTACCCTTGGTTGAAAT-3′; and reverse, 5′-AATGGAGCCACGGCAATCATCATC-3′), α-SMA (forward, 5′-CTGACAGAGGCACCACTGAA-3′; and reverse, 5′-GAAATAGCCAAGCTCAG-3′), and glyceraldehyde-3-phosphate dehydrogenase (forward, 5′-AGTGGGAGTTGCTGTTGAAATC-3′; and reverse, 5′-TGCTGAGTATGTCGTGGAGTCTA-3′).

Western Blot Analysis

The cell extracts were prepared in radioimmunoprecipitation assay buffer, protein concentration in the extracts was determined by Bradford protein assay kit (Bio-Rad, Hercules, CA), and approximately 30 μg of protein was separated by SDS-PAGE. After transferring to nitrocellulose membranes, immunoblots were probed separately with various primary antibodies after blocking with 5% skimmed milk in Tris-buffered saline. Fluorescently labeled secondary antibodies were used for detection by the Odyssey Infrared Imaging System (LI-COR, Inc., Lincoln, NE).

Transmission Electron Microscopy

Mice were sacrificed at 3 days after UUO or sham operation. The kidneys were perfused with PBS and fixed by immersion in 0.1 mol/L cacodylate buffer containing 2.5% glutaraldehyde. Samples were dehydrated through ascending grades of ethanol, embedded, divided into sections (90 nm thick), and stained with lead citrate and 2% aqueous uranyl acetate. They were dehydrated through ascending grades of ethanol. Samples were examined with the JEM-1200 transmission electron microscope (JEOL, Peabody, MA) in the Baylor College of Medicine core facility.

Qualitative Evaluation of Vascular Permeability by Injection of Evans Blue Dye

Vascular permeability was determined by intravascular injection of Evans Blue Dye (Sigma-Aldrich). Evans Blue Dye (20 μg/g mouse body weight and 2 mg/mL in 0.9% NaCl) was injected into the mouse jugular vein. After 30 minutes, dye remaining in the vessels was washed out by perfusing the mouse with 0.9% NaCl via a needle inserted into the left ventricle of the heart. The mouse was then euthanized immediately, and the kidneys were removed. Each kidney was cut into two pieces along the horizontal plane, and both pieces were weighed. One piece was used for Evans Blue Dye extraction with 100% formamide (4 mL/g wet kidney weight) at room temperature for 24 hours. The other piece was dried for 24 hours at 55°C and weighed to obtain the ratio of dry/wet weight. The extracted dye was measured by spectrophotometry (absorbance at 620 nm) using a 96-well plate reader. The results were calculated from a standard curve of Evans Blue Dye (0.05 to 50 μg/mL) and expressed as μg/g dry kidney weight.

Cell Culture and Transfections

HUVECs were purchased from Lonza (Basel, Switzerland). Cells were cultured in Clonetics MEGM Bullet Kit media (Lonza) and starved of supplement growth factors for 24 hours before stimulation with reagents. All assays were performed between passages 4 and 8. TNF-α (Sigma-Aldrich) was used at a dose of 20 ng/mL, and recombinant VEGF (C-1; Santa Cruz Biotechnology) was used at 10 ng/mL. For RNA silencing of the IGF-1R in cells, predesigned Silencer Select siRNAs for human IGF-1R and negative control (none targeting siRNA) were purchased from Thermo Scientific (Waltham, MA). Transfection was done with Lipofectamine 2000 (Life Technologies, Grand Island, NY), according to the manufacturer's instructions. Briefly, cells were seeded at 1×10^6 cells per 6-well plate and incubated for 24 hours. A mixture was prepared of 50 pmol siRNA with 5 μL of Lipofectamine 2000 and added to the culture drop by drop. After 24 hours of transfection, medium was changed to normal medium containing antibiotics. Cells were either treated after 24 hours at 90% to 95% confluence or as otherwise stated. RNA was extracted 24 hours after transfection for real-time RT-PCR analyses, and cell lysates were prepared 48 hours after transfection for Western blot analyses.

In Vitro Permeability Assay

Confluent HUVECs were seeded on 1% gelatin-coated Transwell inserts (0.4-μm pore size; Becton Dickinson, Franklin Lakes, NJ) in 12-well plates and cultured in the upper chamber. At the start of the experiment, HUVECs were transfected with siRNA—IGF-1R or nonrelated scrambled siRNA, or infected with adenovirus (Ad)—IGF-1R, and cultured for 24 to 72 hours. Afterward, 20 μg/mL FITC-dextran (4-kDa relative molecular mass; Sigma-Aldrich) was added to the upper chamber after HUVECs were pretreated with 100 μmol/L H_2O_2 for 1 hour at 37°C. The medium (100 μL) was taken from the lower

compartment every 1 hour and measured using the Tecan microplate reader (excitation, 480 nm; emission, 530 nm).

Renal Microvascular EC Isolation

The method used to isolate the renal microvascular ECs was adapted from that described by Jackson et al.[21] We used anti−PECAM-1 ferrous Dynabeads (Invitrogen, Carlsbad, CA) to immunomagnetically separate the ECs from the other cells present in the renal cortex.[22]

Transmigration of BMCs

The BMCs were isolated from male C57BL/6 mice, as described.[19] HUVECs were transfected with siRNA−IGF-1R or nonrelated scrambled siRNA for 48 hours, or infected with Ad−IGF-1R. HUVECs were cultured in proprietary medium (PromoCell) until confluence in porous filter inserts (5-μm pore size Transwell; Corning, Corning, NY) and activated for 6 hours with 100 μmol/L H_2O_2. After 6 hours, the medium was replaced and BMCs (2×10^6 in 100 μL) were added. The BMCs were subsequently allowed to transmigrate for 2 hours in a humidified CO_2 incubator at 37°C. The transmigrated BMCs were quantified by microscopy (Nikon, Tokyo, Japan).

Statistical Analysis

All data are presented as the means ± SEM. Comparison between groups was made using one-way analysis of variance, followed by pairwise comparisons with P value adjustment; $P < 0.05$ was considered to be statistically significant.

Results

Endothelial-Specific KO of IGF-1R Induces Interstitial Fibroblast Accumulation after UUO

We found that the protein level of IGF-1R was dramatically decreased in kidneys of UUO mice at days 3 and 7 as compared to untreated control kidneys (Figure 1, A and B). Similarly, in a renal IRI model, IGF-1R expression was dramatically decreased at 3 days after IRI and recovered to normal levels by day 7 (Figure 1C). Our results were consistent with a previously reported decrease in mRNA expression of IGF-1R in the rat IRI model.[23] To investigate whether the level of IGF-1R expression in ECs modulates UUO-induced renal fibrosis, mice with EC-specific KO of IGF-1R (VE-Cre$^+$/IGF-1R$^{f/f}$, IGF-1R KO) were generated by crossing IGF-1R−floxed mice with VE-cadherin-Cre transgenic mice (Figure 1D). The IGF-1R KO mice had decreased levels of IGF-1R protein when compared with WT mice (Figure 1E). Immunohistochemical analysis revealed a marked decrease of IGF-1R expression in the ECs of the renal arteriole from IGF-1R KO mice (Figure 1F). To further evaluate the efficiency of VE-cadherin-Cre, we used RFP^{flox}-GFP/VE-cadherin-Cre reporter mice to express GFP in VE-cadherin-Cre−positive cells.[14] The GFP-positive cells were found in the glomerular, peritubular capillaries and arterioles (Figure 1G). These GFP-positive cells also expressed endothelial marker CD31 (Figure 1G), and represent approximately 85.5% ± 2.79% of total CD31-positive cells (Figure 1H). This result indicates that VE-cadherin-Cre expresses functional Cre in ECs in kidneys.

To determine whether IGF-1R in vascular ECs contributes to renal fibrosis, we performed UUO in IGF-1R KO mice. IGF-1R$^{f/f}$ littermates were used as controls. The expressions of α-SMA and PDGFR-α were monitored to represent myofibroblast accumulation. After UUO, the protein and mRNA levels of PDGFR-α and α-SMA were increased, an effect that was further enhanced in the kidneys of IGF-1R KO mice (Figure 1, I and J). Immunostaining results indicated that KO of IGF-1R in ECs increased the number of interstitial fibroblasts (α-SMA$^+$ and PDGFR-α$^+$ cells) in the obstructed kidney versus that of WT mice (Figure 1, K and L).

Exaggeration of Tubulointerstitial Fibrosis in IGF-1R−Deficient Mice

After UUO, blood samples were harvested for serum creatinine content measurements. The levels of serum creatinine in IGF-1R KO mice were not statistically significantly different from WT mice after UUO (Figure 2A), indicating that the contralateral (unobstructed) kidney sufficed for normal excretion. Several renal pathological phenotypes could be observed in both IGF-1R KO and WT mice after UUO. These alterations include tubular atrophy, infiltration of leukocytes, the expanded tubular interstitial volume, and the overaccumulation of the extracellular matrix (Figure 2, B and C). Mice with endothelial KO of IGF-1R displayed significantly severe tubular injury, as determined histologically and by pathological scoring of tubular injury. The degree of injury was similar for both IGF-1R KO and WT mice 7 days after UUO, as indicated by the dilation of tubular lumens in obstructed kidneys (Figure 2B). However, interstitial collagen deposition on Masson's trichrome−stained (Figure 2C) and Picro-Sirius Red sections (Figure 2, D and E) was significantly higher in IGF-1R KO mice versus WT mice. No significant histological abnormality or fibrosis was observed in the sham control (Figure 2, C−E).

Oxidative stress can induce renal apoptosis and contribute to the pathogenesis of the kidney after UUO. On days 1 and 7 after UUO, we measured the renal reactive oxygen species (ROS) measurement *in vivo* by the Fox assay on a chemiluminescence analyzer. We found that significantly increased ROS occurred after 24 hours of UUO in the kidney, but the increased ROS levels were not significantly different between WT and IGF-1R KO mice. However, on day 7, the level of H_2O_2 in IGF-1R KO mice was significantly higher in the UUO group compared to WT mice

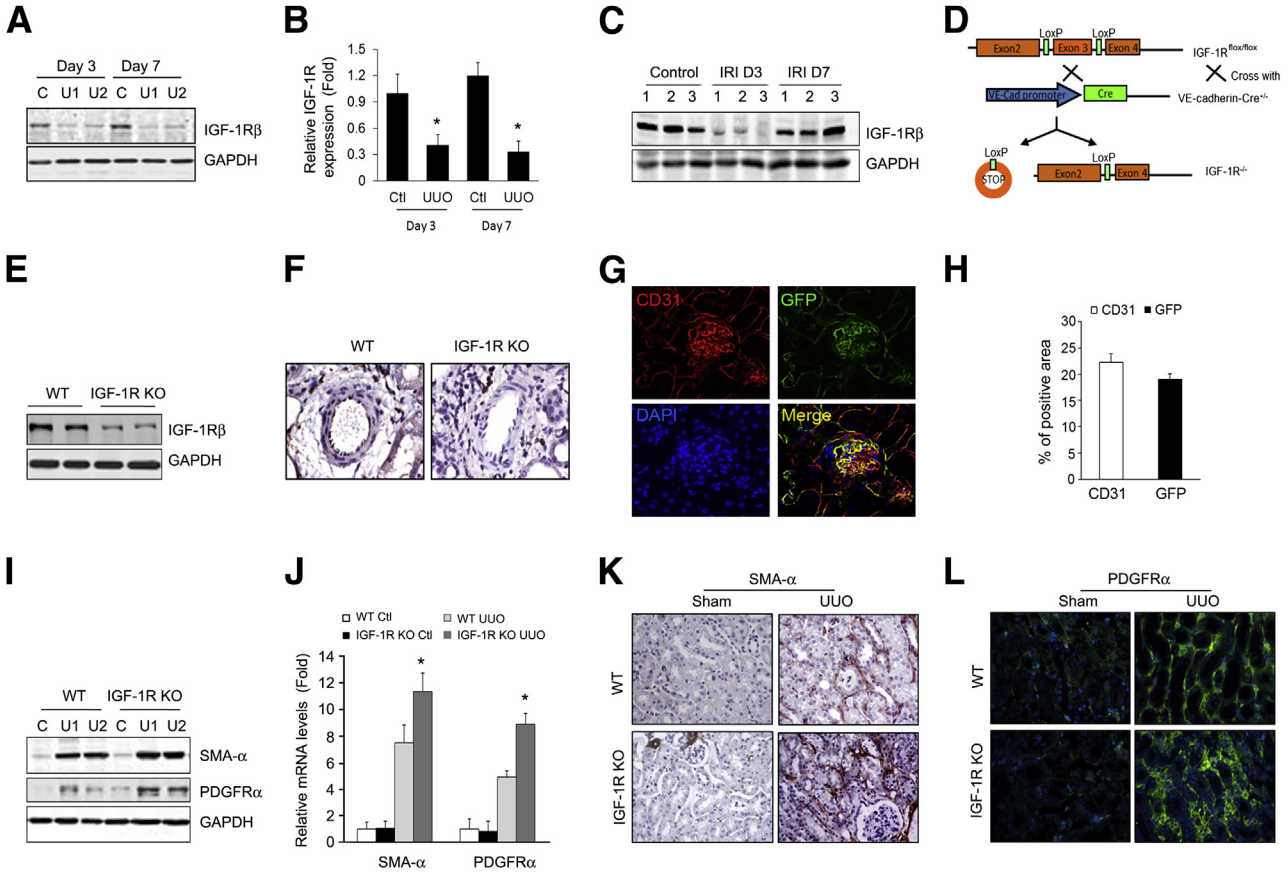

Figure 1 Insulin-like growth factor-1 receptor (IGF-1R) knockout (KO) in endothelial cell (EC) increases unilateral ureteral obstruction (UUO)—induced myofibroblast accumulation. **A:** Determination of total IGF-1R levels in mouse kidneys. Protein was prepared from sham control (C) and obstructed kidneys of wild-type (WT) mice. The level of IGF-1R was determined by Western blot analysis. **B:** Density analysis of IGF-1R protein levels in **A**. **C:** Representative Western blot analysis of total IGF-1R levels in ischemia/reperfusion injury (IRI) kidneys. **D:** Strategy used to generate mice with EC-specific KO of IGF-1R. IGF-1R$^{f/f}$ mice were crossed with vascular endothelial—cadherin (VE-Cad)—Cre^{+} mice to generate IGF-1R$^{f/f}$/VE-cadherin-Cre^{+} mice (IGF-1R KO). **E:** Detection of IGF-1R expression by Western blot analysis from kidneys of WT and IGF-1R KO mice. **F:** IGF-1R staining of renal vessels. Renal tissues were collected from WT mice and IGF-1R KO mice. IGF-1R was detected by immunostaining (brown). **G:** VE-cadherin-Cre/IGF-1R$^{f/f}$ mice were crossed to double-fluorescent Cre reporter mice. Green fluorescent protein (GFP) represents the activity of Cre recombinase. Representative image of costaining of CD31 (red, pseudocolor) and GFP. **H:** Quantification of CD31- and GFP-positive areas. **I** and **J:** Myofibroblast accumulation increases in IGF-1R KO mice after UUO. Myofibroblast cell markers α-smooth muscle actin (SMA) and platelet-derived growth factor receptor (PDGFR)-α were detected by Western blot analysis (**I**), real-time RT-PCR (**J**), and immunostaining (**K** and **L**). *$P < 0.05$. $n = 5$ (**B**); $n = 3$ (**C**); $n = 6$ (**I**—**L**). Ctl, control; GAPDH, glyceraldehyde-3-phosphate dehydrogenase; U1, UUO sample from animal 1; U2, UUO sample from animal 2.

(Figure 2F). Our data suggest that similar oxidative stress was initiated in WT and IGF-1R KO mice after UUO.

Moreover, the expression levels of matrix protein collagen I and fibronectin were detected by Western blot analysis. Consistently, the results showed that IGF-1R KO mice had a significantly higher expression of these proteins in the obstructed kidney versus the expression in WT mice after UUO (Figure 2G). The density analysis revealed a significant difference in protein expression between WT and IGF-1R KO mice (Figure 2, H and I).

IGF-1R KO Mice Display Exaggerated Tubulointerstitial Inflammation after UUO

Inflammation is a critical factor in the development of renal fibrosis. The obstructed kidneys in IGF-1R KO mice show severe infiltration of inflammatory cells with interstitial area extension, especially interstitial area surrounding the vessels, by periodic acid—Schiff staining (Figure 3A). Consistent with the increase in infiltration of inflammatory cells, mRNA expression of the IL-1β, inducible nitric oxide synthase, transforming growth factor-β1, and monocyte chemoattractant protein-1 genes was significantly up-regulated in the kidneys of IGF-1R KO mice compared with that of WT mice after UUO (Figure 3B). To determine whether the preserved renal architecture was associated with an increase in inflammation, we performed immunohistochemistry analysis. Probing for the pan-leukocyte marker CD45, we determined that the IGF-1R KO in ECs resulted in a significant increase in leukocyte infiltration at 3 and 7 days after UUO as compared with WT (Figure 3C). Image analysis of CD45 staining confirmed a significant increase in leukocyte infiltration in the IGF-1R KO mice (Figure 3D). The leukocyte populations presented within injured kidneys consisted primarily of F4/80-positive macrophages, which were increased in IGF-1R KO mice at 3 and 7 days after UUO (Figure 3, E and F). Together, these data

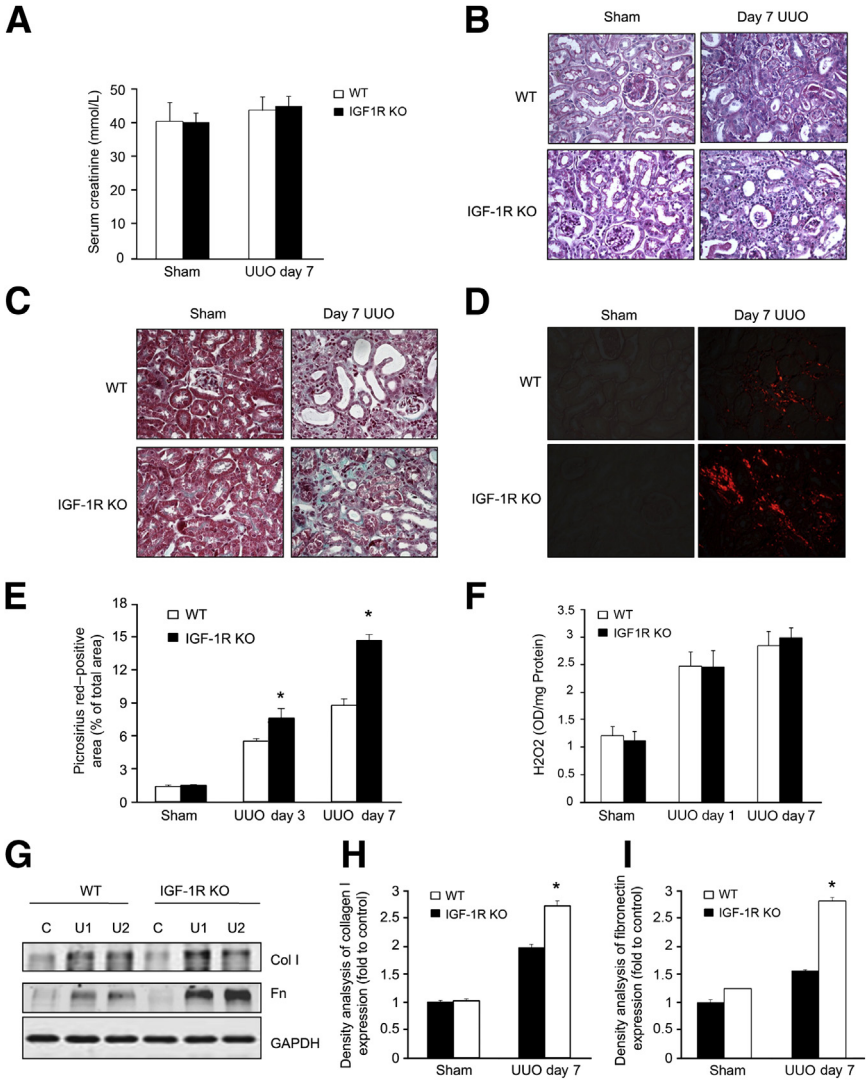

Figure 2 Endothelial knockout (KO) of insulin-like growth factor-1 receptor (IGF-1R) exacerbates renal fibrosis in unilateral ureteral obstruction (UUO). **A:** The Src levels were determined in wild-type (WT) and IGF-1R KO mice after UUO. **B:** Periodic acid—Schiff staining demonstrates dilation of the tubular lumen and thickness of basement membrane of tubules in WT and IGF-1R KO mice. **C:** Masson trichrome staining shows interstitial collagen deposition (blue) in kidneys from mice subjected to UUO. **D:** Enhanced collagen synthesis and deposition are shown by Picro-Sirius Red staining. **E:** The relative density analysis of Picro-Sirius Red—stained sections, such as those shown in **D**. **F:** Hydrogen peroxide (H_2O_2) production in kidney lysates at 1 and 7 days after UUO. **G:** Extracellular matrix collagen (Col) and fibronectin (Fn) were detected by Western blot analysis. **H** and **I:** The results from quantification of these images by computer-assisted image analysis, expressed as percentage of the positive area. Data are given as means ± SEM (**A**, **E**, **F**, **H**, and **I**). $n \geq 6$ mice (**A**, **E**, **F**, **H**, and **I**). $^*P < 0.05$. C, control; GAPDH, glyceraldehyde-3-phosphate dehydrogenase; U1, UUO sample from animal 1; U2, UUO sample from animal 2.

suggest that the proinflammatory response after UUO was exaggerated in IGF-1R KO mice as compared to WT mice.

IGF-1R KO in VE-Cadherin Lineage Hematopoietic Cells Does Not Involve UUO-Induced Pathological Changes

Because of the expression profile of the VE-cadherin promoter, Cre activation in the VE-cadherin-Cre mice occurs not only in the ECs, but also in the hematopoietic cells.[24] To evaluate the role of IGF-1R of hematopoietic cells in UUO-induced inflammation and fibrosis, UUO was performed in WT mice that were transplanted with BMCs from WT mice (WT/WT) or IGF-1R$^{f/f}$/VE-cadherin-Cre$^+$ mice (WT/IGF-1R KO). No significant differences in pathological change were found in obstructed kidneys in the two groups. The dilation of tubular lumens (Supplemental Figure S1A) and interstitial collagen deposition (Supplemental Figure S1, B and C) was not significantly different in the obstructed kidneys (7 days after UUO) of WT/IGF-1R KO chimeric mice versus WT/WT mice. Quantification of CD45$^+$ cells showed no significant difference in obstructed kidneys from mice with either WT or IGF-1R$^{f/f}$/VE-cadherin-Cre$^+$ BMCs (Supplemental Figure S1, D and E). Consistently, the protein expression levels of α-SMA and fibronectin were increased to a comparable level in both groups (Supplemental Figure S1F). These results indicate that IGF-1R KO in the ECs, but not in the hematopoietic cells, of a VE-cadherin lineage plays an essential role in the progress of inflammation and fibrosis in the obstructed kidneys.

IGF-1R Deficiency Is Associated with EC Barrier Dysfunction after UUO

We performed transmission electron microscopy to examine the structural alteration of renal capillary ECs in kidneys of WT and IGF-1R KO mice after UUO (Figure 4A). ECs showed more severe loss of the cellular junctions after UUO, with many more cell processes and morphological changes occurring in the IGF-1R KO mice than in the WT mice. VE-cadherin is an important molecular component of

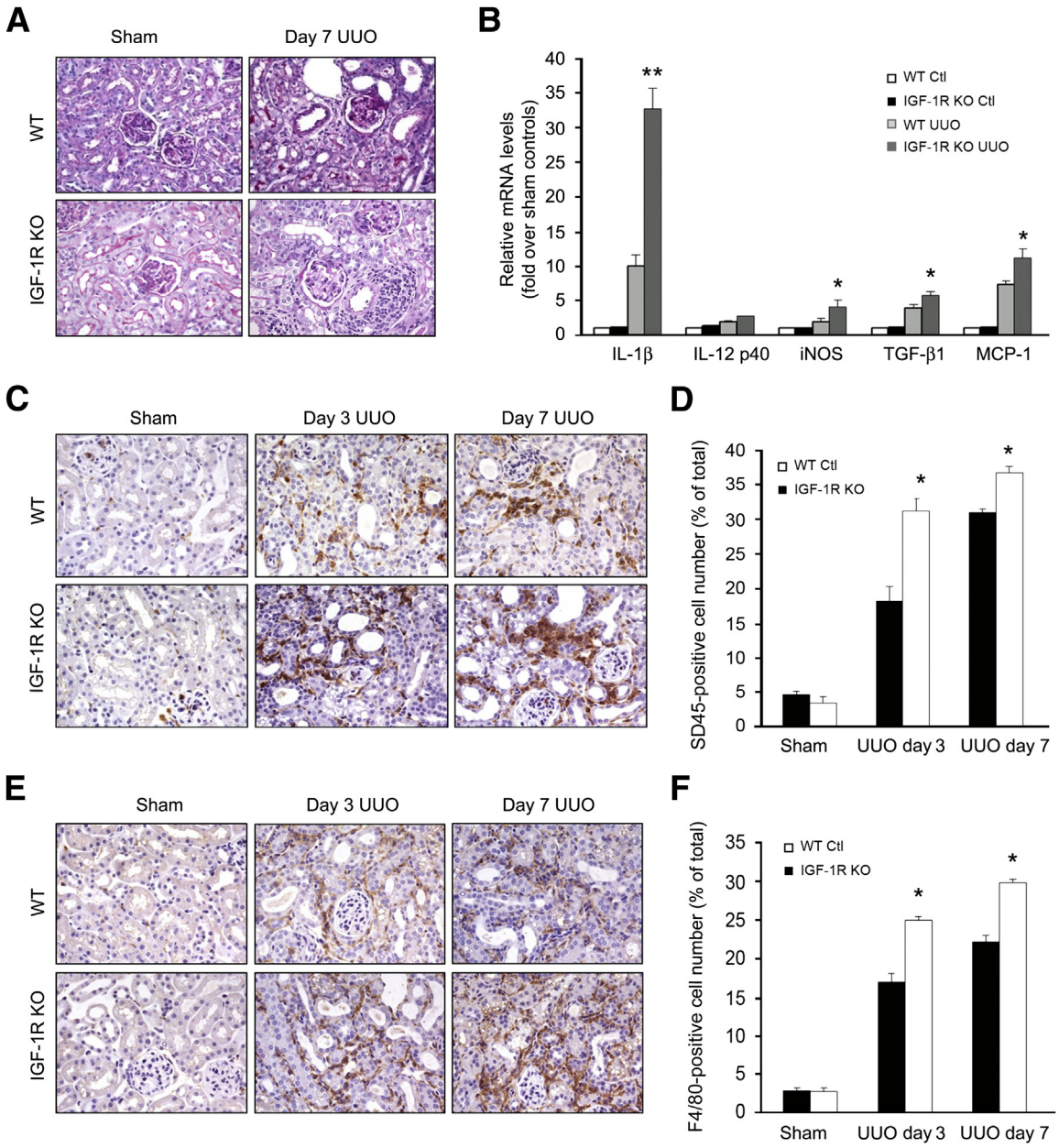

Figure 3 Loss of insulin-like growth factor-1 receptor (IGF-1R) in endothelial cells (ECs) aggravates the inflammation after unilateral ureteral obstruction (UUO). **A:** Periodic acid—Schiff staining shows increased infiltration of inflammatory cells in interstitial and perivascular areas in IGF-1R KO mice at day 7 after UUO. **B:** Deletion of IGF-1R in ECs up-regulates the expression of chemokine genes in the obstructed kidney. Representative real-time PCR analysis and quantitative data are shown. Relative mRNA levels (fold induction over sham controls) were reported after normalization with glyceraldehyde-3-phosphate dehydrogenase (GAPDH). **C:** CD45 immunohistochemistry in kidney sections prepared at 3 and 7 days after UUO. **D:** Quantitative analysis shows a significant increase in the percentage of $CD45^{+}$ cells per field in vascular endothelial (VE)/IGF-$1R^{-/-}$ mice. **E** and **F:** F4/80 expression was detected by immunohistochemistry, and the positive cells were counted. $^{*}P < 0.05$, $^{**}P < 0.01$ versus WT UUO. $n = 6$ (**A**—**F**). Ctl, control; iNOS, inducible nitric oxide synthase; MCP, monocyte chemoattractant protein; TGF, transforming growth factor; WT, wild type.

the capillary endothelial barrier. Increased tyrosine phosphorylation of VE-cadherin correlates with the disassembly of EC junctions.[25] To investigate the role of VE-cadherin in the UUO model, VE-cadherin protein expression and its phosphorylation were measured. We found a significant increase in the amount of tyrosine-phosphorylated VE-cadherin (pVE-cadherin) in obstructed kidneys in the IGF-1R KO mice versus WT mice at day 3 after UUO. The total VE-cadherin showed no significant changes between the two groups (Figure 4B). The ratio of pVE-cadherin/VE-cadherin was greater in the IGF-1R KO mice than that in WT mice (Figure 4C).

Alteration in EC structure and increased phosphorylation of VE-cadherin could lead to vascular leakage. Platelets are the early response cells to EC damage. The platelet-specific marker CD42 gave positive signals along the peritubular

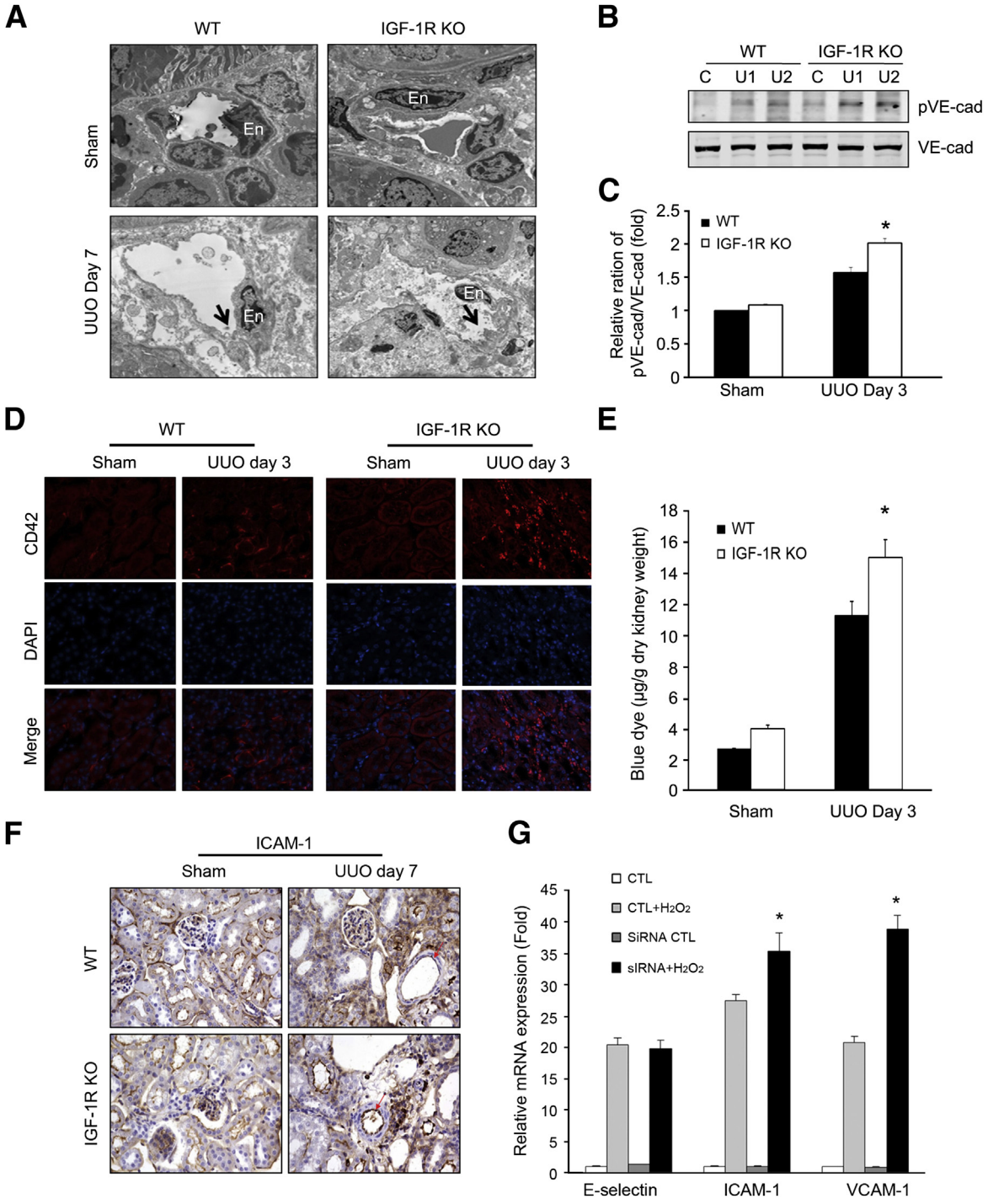

Figure 4 Insulin-like growth factor-1 receptor (IGF-1R) knockout (KO) aggravates endothelial injury and impairs endothelial cell (EC) barrier function in obstructed kidney. **A:** Transmission electron microscopy of peritubular capillaries at day 7 after unilateral ureteral obstruction (UUO) kidney in wild-type (WT) and IGF-1R KO mice. At day 7 after UUO in IGF-1R KO mice, the endothelium of the peritubular capillary (En) is swollen with marked cytoplasmic projections on the surface (**arrows**) in IGF-1R KO mice. **B:** Phosphorylation of vascular endothelial—cadherin (VE-Cad) and total VE-Cad was detected by Western blot analysis after UUO in WT and IGF-1R KO mice. **C:** The ratios of pVE-Cad/total VE-Cad. **D:** Platelet marker CD42 was detected by immunostaining at day 3 after UUO in WT and IGF-1R KO mice. CD42 increases in peritubular capillaries in UUO kidneys from IGF-1R KO mice. **E:** Permeability study performed by injection of Evans Blue Dye. The obstructed left kidney (3 days after UUO) of mice shows Evans Blue Dye accumulation after saline washout, indicating that the obstructed kidneys retain more Evans Blue Dye than the contralateral kidneys. **F:** ICAM-1 expression was detected by immunohistochemistry. **Red arrows** show the ICAM-1 in ECs. **G:** IGF-1R deficiency in human umbilical vein endothelial cells leads to an increase in ICAM-1 and VCAM-1 mRNA expression on hydrogen peroxide (H_2O_2) treatment. Cells were transfected with control (CTL) or small interfering IGF-1R. After 48 hours, cells were treated with 100 μmol/L H_2O_2 for 2 hours and harvested for RT-PCR. Data are given as means ± SEM (**C**). $n = 6$ (**C** and **E**). *$P < 0.05$ pVE-Cad in IGF-1R KO mice versus WT (**C**), Evans Blue Dye in IGF-1R KO mice versus WT (**E**), and mRNA levels in IGF-1R KO mice versus WT (**G**). C, control; U1, UUO sample from animal 1; U2, UUO sample from animal 2.

capillary endothelial lining that increased in the obstructed kidney. Markedly increased staining of CD42 was noted in IGF-1R KO mice compared with WT mice (Figure 4D). To assess the changes in vascular permeability after UUO, the deposition of penetrated Evans Blue Dye was measured after perfusion. Evans Blue Dye levels were greater in the IGF-1R KO mice than in WT mice (Figure 4E).

Because adhesion molecules may play an important role in macrophage recruitment after the oxidative stress after UUO, we detected intercellular adhesion molecule (ICAM)-1 protein expression. Immunohistochemistry staining with an anti−ICAM-1 antibody showed only slight expression of ICAM-1 in the glomerulus, peritubular capillaries, and luminal area of tubule cells in sham control mice, but an increase in ICAM-1 expression was found in the vascular endothelium, tubular epithelium, and interstitial areas in the obstructed kidney from both WT and IGF-1R KO mice. Stronger ICAM-1 expression was apparent in the endothelium of the renal arterioles of IGF-1R KO mice (Figure 4F). Furthermore, we detected the vascular cell adhesion molecule (VCAM)-1, ICAM-1, and E-selectin mRNA expression in HUVECs after treatment with H_2O_2. The *in vitro* experiment showed that H_2O_2 treatment increased the mRNA transcription of VCAM-1, ICAM-1, and E-selectin in ECs and that the increase was greater for VCAM-1 and ICAM-1 in the IGF-1R knockdown HUVECs (Figure 4G). Taken together, our data suggest that IGF-1R in vascular ECs may also be involved in regulating the expression of endothelial adhesion molecules after stimulation due to peroxidative stress.

Knockdown of IGF-1R in HUVECs Increases VE-Cadherin Phosphorylation and Impairs Endothelial Barrier Under Oxidative Stress

VE-cadherin phosphorylation is suppressed under normal conditions, and increased VE-cadherin phosphorylation is associated with increased endothelial barrier dysfunction. Varied proinflammatory factors have been shown to cause endothelial barrier dysfunction. Tyrosine phosphorylation of VE-cadherin in HUVECs was stimulated by different factors, including VEGF, H_2O_2, and TNF-α (Figure 5A). From these factors, we selected H_2O_2 for further study because recent studies have documented an important role for oxidative stress in several renal diseases.[2] H_2O_2 increased tyrosine phosphorylation of VE-cadherin in a time- and dose-dependent manner. H_2O_2 (100 μmol/L) increased pVE-cadherin as early as 15 minutes, with the peak occurring at 30 minutes (Figure 5, B and C).

To investigate the effect of IGF-1R deficiency on H_2O_2-induced phosphorylation of VE-cadherin, IGF-1R expression was knocked down by siRNA (Figure 5D). On H_2O_2 treatment, there was significantly more VE-cadherin phosphorylation in the IGF-1R knockdown cells as compared to the control (small interfering control)−treated HUVECs (Figure 5E). TNF-α or VEGF, which are stressors for producing endogenous H_2O_2,[26,27] markedly enhanced VE-cadherin phosphorylation. Decreased expression of IGF-1R resulted in significantly higher VE-cadherin phosphorylation (Figure 5F). In mouse ECs isolated from WT and IGF-1R KO mice, VE-cadherin was continuously distributed along the cell membrane and well organized. H_2O_2 caused early separation of cell-cell junctions (Figure 5G). IGF-1R deficiency worsened the H_2O_2-induced alterations in IGF-1R KO ECs (Figure 5G). Furthermore, we found that H_2O_2 induced actin polymerization in the membrane ruffles. On stimulation with H_2O_2, the continuation of VE-cadherin on the membrane was broken and showed a punctured pattern in HUVECs. Knockdown of IGF-1R exacerbated the H_2O_2-induced VE-cadherin disruption in HUVECs (Figure 5H).

Evidence for H_2O_2-induced EC permeability includes enhanced dextran-FITC penetration, the loss of IGF-1R−enhanced H_2O_2-induced FITC-dextran leakage, and increased EC permeability when compared to the siRNA control (Figure 5I). Furthermore, knockdown of IGF-1R resulted in augmentation of transendothelial migration of BMCs through the EC monolayers (Figure 5J). Collectively, these data suggest that the phosphorylation of VE-cadherin via IGF-1R signaling was involved in modulation of cytoskeletal remodeling that occurs during endothelial barrier dysfunction.

IGF-1R Stabilizes the Association of VE-PTP with VE-Cadherin

VE-PTP is an endothelial receptor−type phosphatase that regulates tyrosine phosphorylation of VE-cadherin.[28] To address the mechanism of IGF-IR in regulating phosphorylation of VE-cadherin, the association of VE-cadherin with VE-PTP or IGF-1R was determined. In normal conditions, VE-cadherin was associated with VE-PTP in ECs and prevented VE-cadherin phosphorylation. Treatment with H_2O_2 dissociated VE-PTP from VE-cadherin (Figure 6A). Consistently, the pVE-cadherin was increased after H_2O_2 treatment (Figure 6A). In addition, we found that VE-cadherin interacts with IGF-1R (Figure 6A). To test whether IGF-1R is necessary for H_2O_2-induced VE-PTP/VE-cadherin dissociation in ECs, IGF-1R expression was knocked down by siRNA or overexpressed by Ad−IGF-1R infection. The H_2O_2-induced phosphorylation of VE-cadherin was rescued by IGF-1R overexpression, whereas IGF-1R deficiency exacerbated H_2O_2-induced VE-PTP/VE-cadherin dissociation (Figure 6B). Increased IGF-1R expression stabilized the VE-PTP/VE-cadherin complex after H_2O_2 treatment (Figure 6C). Furthermore, overexpression of IGF-1R also inhibited the disruptive effect of H_2O_2 by restoring the linear distribution of the VE-cadherin (Figure 6D). We evaluated the protective effects of IGF-1R overexpression on endothelial barrier integrity. Treatment with Ad−IGF-1R inhibited H_2O_2-induced FITC-dextran leakage and leukocyte transendothelial migration (Figure 6, E and F). These results suggest a novel critical role of IGF-1R

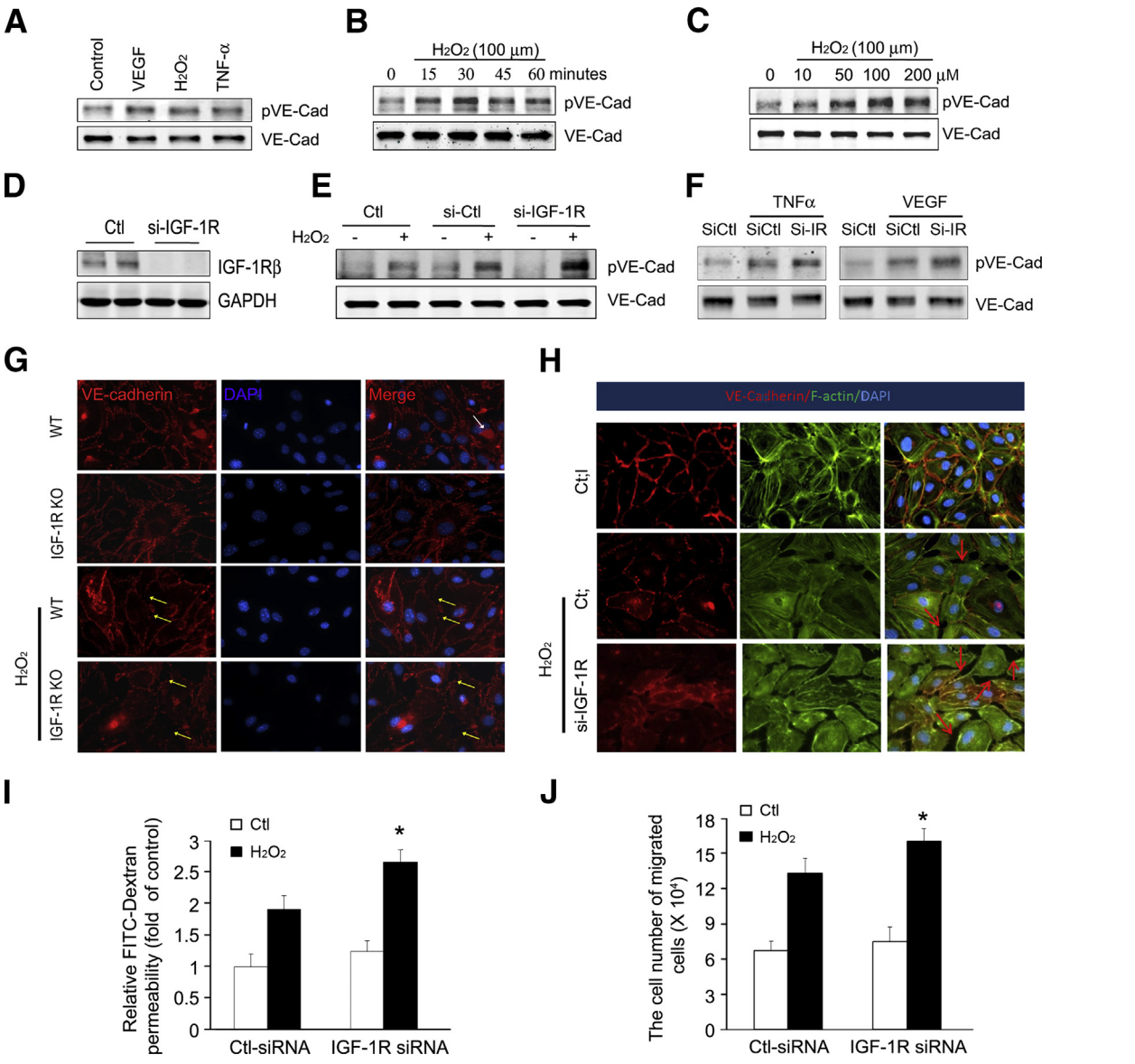

Figure 5 Insulin-like growth factor-1 receptor (IGF-1R) deficiency increases the phosphorylation of vascular endothelial—cadherin (VE-Cad) and impairs endothelial barrier function. **A:** Human umbilical vein endothelial cells (HUVECs) were treated with 50 ng/mL vascular endothelial growth factor (VEGF), 100 μm hydrogen peroxide (H_2O_2), and 10 ng/mL tumor necrosis factor (TNF)-α for 30 minutes. An immunoblot of phospho-Tyr731-VE-Cad was performed. **B** and **C:** H_2O_2 stimulates VE-Cad phosphorylation in a manner that is dependent on both the time of exposure and dose of H_2O_2. HUVECs were stimulated with H_2O_2 at a concentration of 100 μm at the indicated time period (**B**) or for 30 minutes at the indicated H_2O_2 concentration (**C**). **D:** IGF-1R expression in HUVECs was knocked down by IGF-1R siRNA. HUVECs were transfected with 10 nmol/L scrambled siRNA or small interfering (si)—IGF-1R, and the IGF-1R protein level was detected after 48 hours. **E:** IGF-1R deficiency in HUVECs leads to an increase in VE-Cad phosphorylation on H_2O_2 treatment. Cells were transfected with control or si—IGF-1R. After 48 hours of initial transfection, cells were treated with 100 μmol/L H_2O_2 for 30 minutes. Then, cells were harvested for Western blot analysis. **F:** IGF-1R deficiency in HUVECs leads to an increase in VE-Cad phosphorylation after TNF-α and VEGF treatment. Control or si—IGF-1R transfected cells were exposed to TNF-α and VEGF for 30 minutes. Then, cells were harvested for protein lysates and subjected to Western blot analysis. **G:** Mouse ECs isolated from wild-type (WT) and IGF-1R KO mice were fixed and stained with antibodies to VE-cadherin (red). **White arrow** shows the anti—CD31-conjugated Dynabeads. H_2O_2 causes intercellular gap formation (**yellow arrows**). **H:** HUVECs were seeded onto coverslips and transfected with scrambled siRNA or siRNA against IGF-1R. After 48 hours, HUVECs were treated with vehicle or 100 mmol/L H_2O_2 for 30 minutes. Double staining with the F-actin antibody (green) and anti—VE-cadherin antibody (red) was performed. Images were visualized with an immunofluorescence microscope. H_2O_2 stimulation enlarged gaps between the HUVECs. **Red arrows** point to cell-cell junctions with defects in actin-VE-cadherin linkage between adjacent cells. Representative data from three independent experiments are shown. **I:** IGF-1R deficiency enhances endothelial hyperpermeability. Cells were transfected and maintained as above. An *in vitro* Transwell permeability assay was performed, and the amount of fluorescein isothiocyanate (FITC)—dextran diffused to the lower chamber was measured. **J:** IGF-1R KO enhances H_2O_2-induced transendothelial migration. HUVECs were transfected with control or siRNA against IGF-1R. After treating with H_2O_2 for 30 minutes, the medium was replaced and the bone marrow cells were added into the upper chamber. Bone marrow cells in the lower chamber were counted. Data are given as means ± SD (**I** and **J**). *$P < 0.05$. Ctl, control; GAPDH, glyceraldehyde-3-phosphate dehydrogenase.

in preserving cell-cell adhesion and barrier function in HUVECs.

Transposon-Mediated IGF-1R Expression Suppresses UUO-Induced Inflammation and Fibrosis in IGF-1R KO Mice

To explore the potential therapeutic role of IGF-1R in obstructive renal injury, we constructed an IGF-1R expression plasmid under control of the VE-cadherin promoter in a piggyBac transposon vector to obtain the pT-VE-cadherin-IGF-1R construct. It was then transferred into the kidney, which was later subjected to UUO to induce interstitial fibrosis. The gene transfer was accomplished using a transposon system to integrate the *IGF1R* gene into the genomic DNA, so as to achieve long-term gene expression.[16,29] Initially, we confirmed that this system mediates expression of IGF-IR in vascular ECs by immunohistochemical staining (Figure 7A) and Western blot analysis (Figure 7B). The positive immunostaining of IGF-1R was restored in endothelium of renal vessels in mice with IGF-1R overexpression (IGF-1R transposon [Tn]) that was mediated by the transposon system (Figure 7A).

To test whether expression of IGF-1R in ECs influences VE-cadherin phosphorylation, we examined pVE-cadherin from the obstructed kidney in both IGF-1R KO and IGF-1R Tn mice. We found that the extent of VE-cadherin phosphorylation was significantly decreased in IGF-1R Tn mice when compared to IGF-1R KO mice (Figure 7C). We then determined the degree of endothelial leakage by Evans Blue Dye detection. The deposited Evans Blue Dye levels were significantly lower in IGF-1R overexpression mice than in IGF-1R KO mice (Figure 7D).

Notably, there was a significant reduction in inflammatory cell infiltration (leukocyte, $CD45^{+}$; macrophage, $F4/80^{+}$) in the obstructed kidney in IGF-1R Tn mice versus the IGF-1R KO mice after UUO (Figure 7E). Similarly, the UUO-induced increase in chemokines was also significantly suppressed by IGF-1R overexpression (Figure 7F). Periodic acid—Schiff and Picro-Sirius Red staining and quantitative assessment confirmed that IGF-1R overexpression in kidneys resulted in a significant reduction in fibrosis at day 7 of UUO when compared to the IGF-1R KO kidneys (Figure 7, G—K). Consistent with these observations, reduced expression of fibronectin, α-SMA,

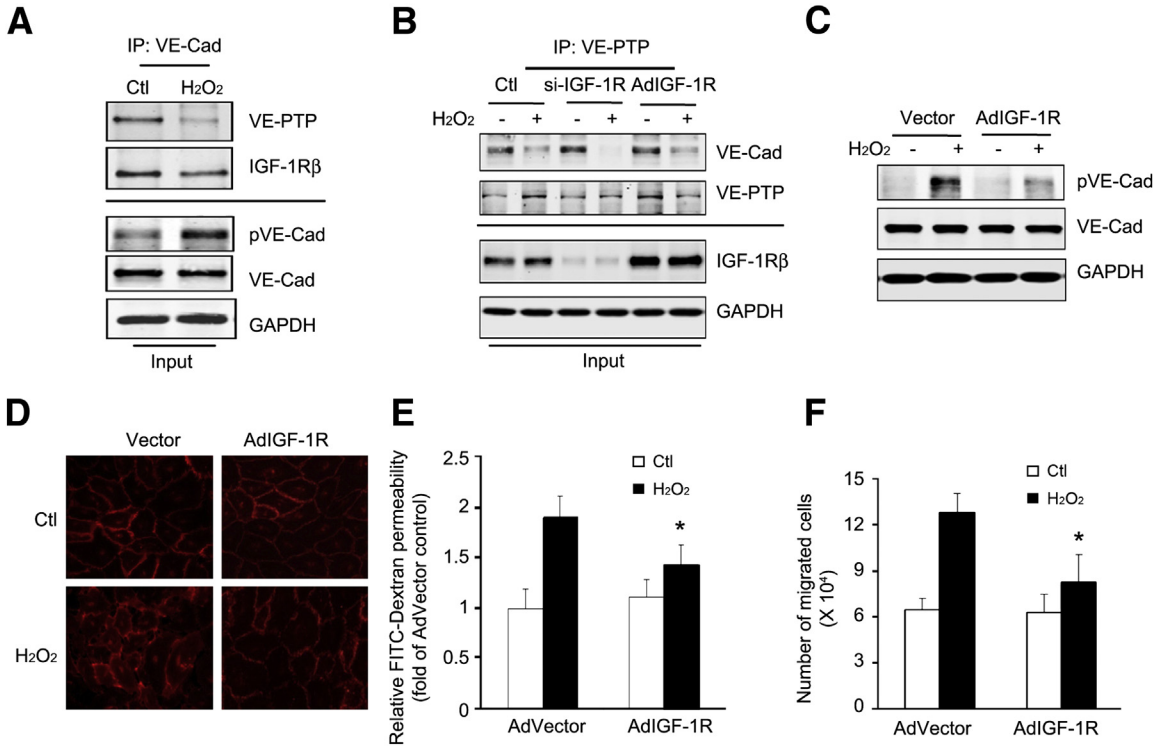

Figure 6 Overexpression of insulin-like growth factor-1 receptor (IGF-1R) enhances interaction between vascular endothelial—cadherin (VE-Cad) and VE—protein tyrosine phosphatase (PTP) and promotes endothelial barrier function. **A:** Hydrogen peroxide (H_2O_2) dissociates VE-Cad from phosphatase VE-PTP. Human umbilical vein endothelial cells (HUVECs) were treated with H_2O_2 for 30 minutes. Immunoprecipitation was performed with anti—VE-Cad antibodies. Immunoprecipitated proteins and the inputs were analyzed by Western blot analysis. **B:** Knockdown of IGF-1R enhances H_2O_2-induced dissociation of VE-cadherin and VE-PTP. HUVECs were transfected with small interfering (si)—IGF-1R or infected with adenovirus (Ad)—IGF-1R for 48 hours, followed by H_2O_2 treatment for 30 minutes. Immunoprecipitation and Western blot analysis were performed. The IGF-1R levels from the input were detected. The data are representative of three independent experiments. **C:** Overexpression of IGF-1R in HUVECs suppresses H_2O_2-induced VE-Cad phosphorylation. **D:** Overexpression of IGF-1R preserves cadherin junction structure. HUVECs were infected with AdVector or Ad—IGF-1R before H_2O_2 treatment. VE-Cad (red) immunostaining was performed. **E** and **F:** Overexpression of IGF-1R protects H_2O_2-induced barrier dysfunction. HUVECs were infected with control or Ad—IGF-1R and treated with H_2O_2. The permeability of fluorescein isothiocyanate (FITC)—dextran (**E**) or transendothelial migration of bone marrow cells (**F**) was determined. Data are representative of three repeated experiments. Data are given as means ± SD (**E** and **F**). $^{*}P < 0.05$. Ctl, control; GAPDH, glyceraldehyde-3-phosphate dehydrogenase.

and collagen I in IGF-1R overexpression mice was found as compared with IGF-1R KO mice (Figure 7, H and I). These data suggest that up-regulation of IGF-1R expression in WT mice serves to limit the increase in renal vascular permeability and positively influences inflammation and fibrosis after UUO.

Discussion

The results of this study confirm that EC damage and endothelial barrier dysfunction are the initial factors in obstructive kidney pathological changes. IGF-1R in ECs shows a protective role in the maintenance of EC barrier

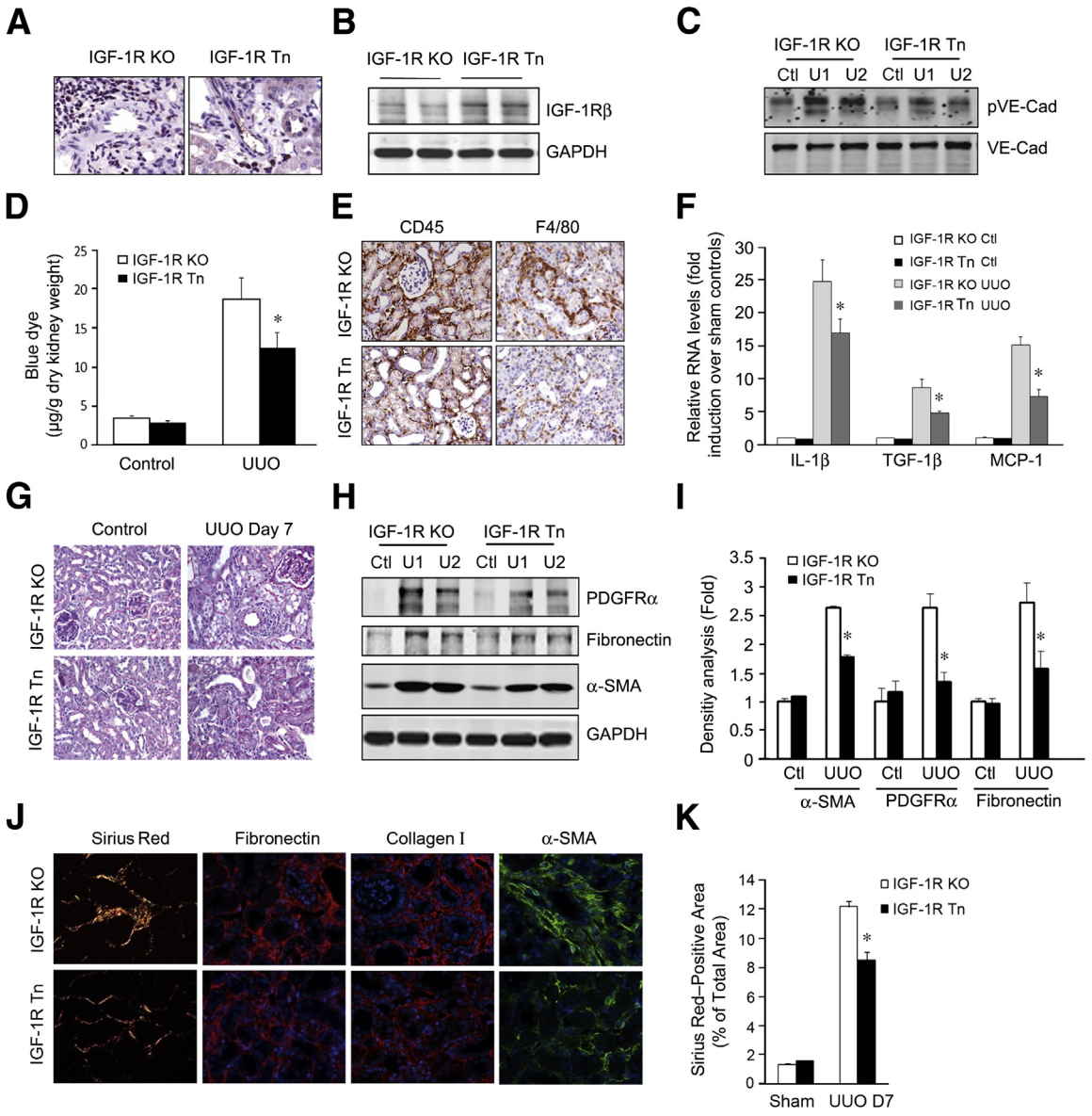

Figure 7 Transposon-mediated insulin-like growth factor-1 receptor (IGF-1R) expression *in vivo* protects against unilateral ureteral obstruction (UUO)—induced inflammatory and fibrogenic responses in IGF-1R knockout mice. **A** and **B:** IGF-1R expression in renal endothelial cells (ECs). IGF-1R expression plasmids were injected into the kidneys of IGF-1R knockout (KO) mice. After 3 days, the IGF-1R expression was determined by immunostaining (**A**) or by Western blot analysis (**B**). **C:** Transposon-delivered IGF-1R expression inhibits vascular endothelial—cadherin (VE-Cad) phosphorylation in IGF-1R KO or IGF-1R transposon (Tn) mice after UUO. **D:** Overexpression of IGF-1R reverses UUO-induced endothelial barrier dysfunction. Evans Blue Dye was injected into IGF-1R KO or IGF-1R Tn mice at day 3 after UUO. The deposited dye was measured by spectrophotometry. **E** and **F:** Overexpression of IGF-1R in ECs suppresses the UUO-induced inflammatory response. **E:** After UUO was performed in both IGF-1R KO or IGF-1R Tn mice, inflammatory cells ($F4/80^+$ and $CD45^+$) were detected in the kidneys. **F:** The expression of chemokines was detected by real-time RT-PCR. **G:** IGF-1R expression reduces UUO-induced fibrosis. Periodic acid—Schiff staining was performed 7 days after UUO. **H** and **I:** The protein levels of myofibroblasts and fibronectin were detected by Western blot analysis (**H**), and the relative density is shown (**I**). **J:** Immunostaining of myofibroblast and fibrosis markers in both the IGF-1R KO or IGF-1R Tn mice after UUO. **K:** Density analysis of Picro-Sirius Red staining in **J**. Data were means ± SEM. $n = 6$ (**A**—**F**). $^*P < 0.05$. Ctl, control; GAPDH, glyceraldehyde-3-phosphate dehydrogenase; PDGFR, platelet-derived growth factor receptor; SMA, smooth muscle actin; U1, UUO sample from animal 1; U2, UUO sample from animal 2.

integrity. Specific KO of IGF-1R in vascular ECs increases permeability and infiltration of inflammatory cells, promoting a significant, progressive, renal interstitial fibrosis in the mouse UUO model of CKD. These changes were associated with a significant increase in VE-cadherin protein phosphorylation. The *in vitro* experiments showed that loss of IGF-1R increased the permeability of the endothelial monolayer after H_2O_2 treatment. This augmented the disruption of the VE-PTP/VE-cadherin complex at adherens junctions, leading to tyrosine phosphorylation of VE-cadherin. Finally, the IGF-1R overexpression in the endothelium resulted in the attenuation of interstitial inflammation and fibrosis. Taken together, the current data indicate that IGF-1R in ECs plays a critical role in the maintenance of vascular integrity via enhancing the stability of VE-cadherin at endothelial junctions.

The endothelial monolayer lies at the interface between blood and the extravascular space, playing a crucial role in vascular homeostasis.[30] Maintaining the functional integrity of the endothelium is important in the prevention or delay of vascular diseases. Endothelial dysfunction is a hallmark of CKD and begins early in the progression of CKD.[31] It has been widely reported that patients with CKD display endothelial dysfunction.[31] In pathological conditions, injury to vascular ECs results in increased permeability of the vascular barrier, with increased extravasation of neutrophils and monocytes across the vessel wall.[32] We found that there was endothelial damage and platelet aggregation in the interstitial capillary in the obstructed kidneys (Figure 4). These indications of a leaky EC barrier were further supported by increased Evans Blue Dye staining in the UUO kidneys (Figure 4E).

There are several potential points that link EC barrier dysfunction with renal fibrosis. ECs are involved in modulating local hemostasis and thrombolysis, producing vasoactive compounds, and providing a nonpermeable barrier preventing local activation and proliferation of local fibroblasts or pericytes.[33] First, the leakage of the endothelium can promote platelet adhesion and aggregation, which is an immediate response to EC damage. Platelets store proinflammation molecules (sphingosine-1-phosphate) and growth factors (PDGF and transforming growth factor-β1) that can affect surrounding fibroblast differentiation and proliferation. Second, extravasation of the inflammatory cells through the impaired endothelial layer causes them to accumulate in the renal interstitial area. There, the inflammatory cells secrete cytokines and chemokines, including monocyte chemoattractant protein-1,[34] stromal cell-derived factor-1,[35] and/or others, that may stimulate myofibroblast proliferation. In this way, the inflammatory cells exert a paracrine effect on surrounding cells.[19] Finally, the endothelial damage could free the coated pericytes, because the hyperplasia of pericytes also leads to renal fibrosis.[36] We conclude that UUO-induced endothelial barrier dysfunction is an initial factor that stimulates inflammatory and fibrogenic responses.

The molecules and factors in CKD that cause endothelial changes are unclear, but it has been reported that treatment of ECs with uremic serum increases the expression of VCAM and tissue factor.[37] Others have suggested that the reduced EC function in CKD is possibly caused by increased oxidative stress in the vascular wall.[38,39] We found that ROS (H_2O_2 and 4-hydroxynonenal) induced EC barrier dysfunction (Figure 4). IGF-1R exerts multiple physiological and pathological effects on the vasculature. Accumulating evidence indicates that IGF-1R is a vascular protective factor.[40,41] It reduces oxidative stress and neuroinflammatory response.[42] Increased IGF-1R improved endothelial progenitor function and promoted endothelial regeneration,[43,44] whereas IGF-1R KO increased diabetes-induced cardiac fibrosis.[45,46] It has been reported that CKD impairs the IGF-1/IGF-1R signaling pathway, leading to dysfunction of muscle regeneration.[47] In conclusion, we found that UUO decreased the expression of IGF-1R in kidney (Figure 1), suggesting that endothelial IGF-1R could play a role in renal fibrosis.

To test this hypothesis, IGF-1R KO and WT mice were subjected to UUO, and their outcomes were compared. The kidneys of IGF-1R KO mice showed a greater increase in vascular permeability, inflammatory cell infiltration, greater accumulation of myofibroblasts, and more deposition of extracellular matrix (Figures 1 and 2). Consequently, loss of IGF-1R in ECs mediated the barrier dysfunction in UUO, which directly promotes fibrosis via the accumulation of inflammatory cells, especially macrophages (Figure 3). UUO-induced accumulation of fibroblasts and tubulointerstitial fibrosis were significantly exacerbated in IGF-1R KO mice (Figures 1 and 2). In addition, these responses were blunted in IGF-1R Tn mice (Figure 7). These findings indicate that vascular endothelium−specific IGF-1R plays a pathological role in the progression of renal inflammation via barrier dysfunction. Infiltration of platelets and inflammatory cells introduced cytokines that are critical mediators of renal fibrosis, such as IL-1β, inducible nitric oxide synthase, and chemokine ligand-2/monocyte chemoattractant protein-1.

VE-cadherin-Cre transgenic mice have been widely used to deliver gene overexpression[48] or knockout[49] in ECs. By using reporter transgenic mice, we found that most of the CD31-positive ECs in the kidney (approximately 85.5% ± 2.79%) were labeled by GFP that was turned on by VE-cadherin-Cre (Figure 1). With the same reporter mice, a recent report showed that VE-cadherin-Cre was active in only 50% of the kidney.[50] This discrepancy could be due to the different methods or antibodies used in the analysis.

The Cre recombinase expressed in the VE-cadherin-Cre transgenic mice was predominantly active in ECs and, in addition, in hematopoietic cells.[24] Therefore, the IGF-1R gene was knocked out in all VE-cadherin−expressing cells (ECs) and their lineages (including some hematopoietic cells). The deteriorative effects on renal fibrosis in IGF-$1R^{f/f}$/VE-cadherin-Cre^{+} mice could be due to dysfunction in the hematopoietic cells of VE-cadherin lineage. However, transplant of BMCs from IGF-$1R^{f/f}$/VE-cadherin-Cre^{+} mice

into WT mice had no observed effects on UUO-induced fibrosis. Therefore, our results indicate that loss of IGF-1R in ECs was the major contributor to the accelerated UUO-induced inflammatory and fibrogenic response.

More important, because VE-cadherin is involved in pericellular vascular permeability,[51,52] we hypothesized that its function may be modulated by IGF-1R. VE-cadherin phosphorylation was measured at the critical tyrosine residue Y-731, a mechanism causing disassembly of this protein from the endothelial junction. Our data indicate that after UUO, decreased IGF-1R in ECs increased VE-cadherin phosphorylation, whereas the overexpression of IGF-1R in the endothelium partially restored its barrier function through decreased phosphorylation of VE-cadherin (Figure 7). It has previously been reported that IGF-1 prevented EC apoptosis by ROS, whereas specific knockout of IGF-1R caused vascular hyperpermeability and increased H_2O_2-induced tissue injury.[53] In cultured ECs, we also observed an increased phosphorylation of VE-cadherin after treatment with H_2O_2, whereas overexpression of Ad−IGF-1R suppressed this response (Figure 6C). These results demonstrate that stabilization of endothelial junctions is a mechanism by which IGF-1R reduces vascular hyperpermeability through reduction of the VE-cadherin phosphorylation. VE-PTP, a VE-cadherin phosphatase in ECs, determines the phosphorylation status of VE-cadherin through direct interaction. Consistently, decreased IGF-1R levels exacerbated the H_2O_2-induced dissociation of the VE-PTP/VE-cadherin complex in ECs, whereas increased IGF-1R expression restored the VE-PTP/VE-cadherin interaction to control levels (Figure 6). Another key finding from our study is the association of the IGF-1R with VE-cadherin in HUVECs. This finding is supported by the co-immunoprecipitation of the IGF-1R with VE-cadherin from HUVEC whole cell lysates (Figure 6). Consistent with our observations, studies have shown that in human colonic mucosa, IGF-1R has been found complexed with E-cadherin.[54] The presence of IGF-1R complexed with E-cadherin at points of cell-cell contact in corneal epithelial cells has also been identified.[54] A decrease in IGF-1R expression led to a decreased amount of the E-cadherin−catenin complex, causing a defect in the epithelial barrier. These studies suggest that IGF-1R plays a role in the stabilization of E-cadherin−catenin complex in breast cancer cells.[55] Our results strongly support the interplay between the IGF-1R and VE-PTP/VE-cadherin complex in maintenance of the cell-cell contact of HUVECs in the absence of exogenous IGF-1. Further studies are needed to investigate the regulatory pathways.

In summary, our study confirms the critical role of IGF-1R in regulation of the stability of the VE-PTP/VE-cadherin complex, thereby affecting the phosphorylation state of VE-cadherin. Through this mechanism, we found that decreased IGF-1R expression impaired endothelial barrier function at the interendothelial junctions after UUO.

Acknowledgments

M.L., L.E.W., A.L., and J.L. performed experiments, designed the study, and analyzed the data; M.L., W.E.M., and J.C. performed a literature search and interpreted the data; M.H.W. provided critical reagents and interpreted the data; M.L., L.E.W., and J.C. wrote the manuscript; M.L., L.E.W., A.L., J.L., M.H.W., W.E.M., and J.C. had final approval of the submitted and published manuscript.

Supplemental Data

Supplemental material for this article can be found at *http://dx.doi.org/10.1016/j.ajpath.2015.01.027*.

References

1. Collins AJ, Foley RN, Herzog C, Chavers BM, Gilbertson D, Ishani A, et al: Excerpts from the US Renal Data System 2009 Annual Data Report. Am J Kidney Dis 2010, 55:S1−S420. A426-427
2. Feletou M, Vanhoutte PM: Endothelial dysfunction: a multifaceted disorder (the wiggers award lecture). Am J Physiol Heart Circ Physiol 2006, 291:H985−H1002
3. Deanfield JE, Halcox JP, Rabelink TJ: Endothelial function and dysfunction: testing and clinical relevance. Circulation 2007, 115: 1285−1295
4. Kim W, Moon SO, Lee SY, Jang KY, Cho CH, Koh GY, Choi KS, Yoon KH, Sung MJ, Kim DH, Lee S, Kang KP, Park SK: Comp-angiopoietin-1 ameliorates renal fibrosis in a unilateral ureteral obstruction model. J Am Soc Nephrol 2006, 17:2474−2483
5. Pollak M: Insulin-like growth factor physiology and cancer risk. Eur J Cancer 2000, 36:1224−1228
6. Mitsui R, Fujita-Yoshigaki J, Narita T, Matsuki-Fukushima M, Satoh K, Qi B, Guo MY, Katsumata-Kato O, Sugiya H: Maintenance of paracellular barrier function by insulin-like growth factor-I in submandibular gland cells. Arch Oral Biol 2010, 55:963−969
7. Chisalita SI, Arnqvist HJ: Insulin-like growth factor I receptors are more abundant than insulin receptors in human micro- and macrovascular endothelial cells. Am J Physiol Endocrinol Metab 2004, 286: E896−E901
8. Pandini G, Frasca F, Mineo R, Sciacca L, Vigneri R, Belfiore A: Insulin/insulin-like growth factor I hybrid receptors have different biological characteristics depending on the insulin receptor isoform involved. J Biol Chem 2002, 277:39684−39695
9. Paneni F, Beckman JA, Creager MA, Cosentino F: Diabetes and vascular disease: pathophysiology, clinical consequences, and medical therapy: part I. Eur Heart J 2013, 34:2436−2443
10. Spoerri PE, Ellis EA, Tarnuzzer RW, Grant MB: Insulin-like growth factor: receptor and binding proteins in human retinal endothelial cell cultures of diabetic and non-diabetic origin. Growth Horm IGF Res 1998, 8:125−132
11. Dejana E, Orsenigo F, Lampugnani MG: The role of adherens junctions and VE-cadherin in the control of vascular permeability. J Cell Sci 2008, 121:2115−2122
12. Cheng J, Du J: Mechanical stretch simulates proliferation of venous smooth muscle cells through activation of the insulin-like growth factor-1 receptor. Arterioscler Thromb Vasc Biol 2007, 27: 1744−1751
13. Holzenberger M, Dupont J, Ducos B, Leneuve P, Geloen A, Even PC, Cervera P, Le Bouc Y: Igf-1 receptor regulates lifespan and resistance to oxidative stress in mice. Nature 2003, 421:182

14. Liang M, Liang A, Wang Y, Jiang J, Cheng J: Smooth muscle cells from the anastomosed artery are the major precursors for neointima formation in both artery and vein grafts. Basic Res Cardiol 2014, 109:431
15. Saridey SK, Liu L, Doherty JE, Kaja A, Galvan DL, Fletcher BS, Wilson MH: Piggybac transposon-based inducible gene expression in vivo after somatic cell gene transfer. Mol Ther 2009, 17: 2115−2120
16. Liang A, Wang Y, Woodard LE, Wilson MH, Sharma R, Awasthi YC, Du J, Mitch WE, Cheng J: Loss of glutathione S-transferase A4 accelerates obstruction-induced tubule damage and renal fibrosis. J Pathol 2012, 228:448−458
17. Cheng J, Truong LD, Wu X, Kuhl D, Lang F, Du J: Serum- and glucocorticoid-regulated kinase 1 is upregulated following unilateral ureteral obstruction causing epithelial-mesenchymal transition. Kidney Int 2010, 78:668−678
18. Liang A, Wang Y, Han G, Truong L, Cheng J: Chronic kidney disease accelerates endothelial barrier dysfunction in a mouse model of an arteriovenous fistula. Am J Physiol Renal Physiol 2013, 304: F1413−F1420
19. Cheng J, Wang Y, Liang A, Jia L, Du J: Fsp-1 silencing in bone marrow cells suppresses neointima formation in vein graft. Circ Res 2012, 110:230−240
20. Nappi AJ, Vass E: Hydrogen peroxide production in immune-reactive drosophila melanogaster. J Parasitol 1998, 84:1150−1157
21. Jackson CJ, Garbett PK, Nissen B, Schrieber L: Binding of human endothelium to Ulex europaeus I-coated Dynabeads: application to the isolation of microvascular endothelium. J Cell Sci 1990, 96(Pt 2): 257−262
22. McGinn S, Poronnik P, Gallery ED, Pollock CA: A method for the isolation of glomerular and tubulointerstitial endothelial cells and a comparison of characteristics with the human umbilical vein endothelial cell model. Nephrology (Carlton) 2004, 9:229−237
23. Fernández M, Medina A, Santos F, Carbajo E, Rodriguez J, Alvarez J, Cobo A: Exacerbated inflammatory response induced by insulin-like growth factor I treatment in rats with ischemic acute renal failure. J Am Soc Nephrol 2001, 12:1900−1907
24. Alva JA, Zovein AC, Monvoisin A, Murphy T, Salazar A, Harvey NL, Carmeliet P, Iruela-Arispe ML: VE-Cadherin-Cre-recombinase transgenic mouse: a tool for lineage analysis and gene deletion in endothelial cells. Dev Dyn 2006, 235:759−767
25. Orsenigo F, Giampietro C, Ferrari A, Corada M, Galaup A, Sigismund S, Ristagno G, Maddaluno L, Koh GY, Franco D, Kurtcuoglu V, Poulikakos D, Baluk P, McDonald D, Grazia Lampugnani M, Dejana E: Phosphorylation of VE-cadherin is modulated by haemodynamic forces and contributes to the regulation of vascular permeability in vivo. Nat Commun 2012, 3:1208
26. Monaghan-Benson E, Burridge K: The regulation of vascular endothelial growth factor-induced microvascular permeability requires rac and reactive oxygen species. J Biol Chem 2009, 284:25602−25611
27. Nwariaku FE, Liu Z, Zhu X, Nahari D, Ingle C, Wu RF, Gu Y, Sarosi G, Terada LS: NADPH oxidase mediates vascular endothelial cadherin phosphorylation and endothelial dysfunction. Blood 2004, 104:3214−3220
28. Hayashi M, Majumdar A, Li X, Adler J, Sun Z, Vertuani S, Hellberg C, Mellberg S, Koch S, Dimberg A, Koh GY, Dejana E, Belting HG, Affolter M, Thurston G, Holmgren L, Vestweber D, Claesson-Welsh L: VE-PTP regulates VEGFR2 activity in stalk cells to establish endothelial cell polarity and lumen formation. Nat Commun 2013, 4:1672
29. Wilson MH, Coates CJ, George AL Jr: Piggybac transposon-mediated gene transfer in human cells. Mol Ther 2007, 15:139−145
30. Cines DB, Pollak ES, Buck CA, Loscalzo J, Zimmerman GA, McEver RP, Pober JS, Wick TM, Konkle BA, Schwartz BS, Barnathan ES, McCrae KR, Hug BA, Schmidt AM, Stern DM: Endothelial cells in physiology and in the pathophysiology of vascular disorders. Blood 1998, 91:3527−3561
31. Jourde-Chiche N, Dou L, Cerini C, Dignat-George F, Brunet P: Vascular incompetence in dialysis patients: protein-bound uremic toxins and endothelial dysfunction. Semin Dial 2011, 24:327−337
32. Libby P, Ridker PM, Maseri A: Inflammation and atherosclerosis. Circulation 2002, 105:1135−1143
33. Schrimpf C, Xin C, Campanholle G, Gill SE, Stallcup W, Lin SL, Davis GE, Gharib SA, Humphreys BD, Duffield JS: Pericyte TIMP3 and ADAMTS1 modulate vascular stability after kidney injury. J Am Soc Nephrol 2012, 23:868−883
34. Furukawa Y, Matsumori A, Ohashi N, Shioi T, Ono K, Harada A, Matsushima K, Sasayama S: Anti−monocyte chemoattractant protein-1/monocyte chemotactic and activating factor antibody inhibits neointimal hyperplasia in injured rat carotid arteries. Circ Res 1999, 84:306−314
35. Zernecke A, Schober A, Bot I, von Hundelshausen P, Liehn EA, Möpps B, Mericskay M, Gierschik P, Biessen EA, Weber C: SDF-1α/CXCR4 axis is instrumental in neointimal hyperplasia and recruitment of smooth muscle progenitor cells. Circ Res 2005, 96:784−791
36. Bjarnegård M, Enge M, Norlin J, Gustafsdottir S, Fredriksson S, Abramsson A, Takemoto M, Gustafsson E, Fässler R, Betsholtz C: Endothelium-specific ablation of PDGFB leads to pericyte loss and glomerular, cardiac and placental abnormalities. Development 2004, 131:1847−1857
37. Serradell M, Diaz-Ricart M, Cases A, Zurbano MJ, Lopez-Pedret J, Arranz O, Ordinas A, Escolar G: Uremic medium causes expression, redistribution and shedding of adhesion molecules in cultured endothelial cells. Haematologica 2002, 87:1053−1061
38. Vaziri ND, Ni Z, Oveisi F, Liang K, Pandian R: Enhanced nitric oxide inactivation and protein nitration by reactive oxygen species in renal insufficiency. Hypertension 2002, 39:135−141
39. Wever R, Boer P, Hijmering M, Stroes E, Verhaar M, Kastelein J, Versluis K, Lagerwerf F, van Rijn H, Koomans H, Rabelink T: Nitric oxide production is reduced in patients with chronic renal failure. Arterioscler Thromb Vasc Biol 1999, 19:1168−1172
40. Delafontaine P, Song YH, Li Y: Expression, regulation, and function of IGF-1, IGF-1R, and IGF-1 binding proteins in blood vessels. Arterioscler Thromb Vasc Biol 2004, 24:435−444
41. Conti E, Carrozza C, Capoluongo E, Volpe M, Crea F, Zuppi C, Andreotti F: Insulin-like growth factor-1 as a vascular protective factor. Circulation 2004, 110:2260−2265
42. Nadjar A, Berton O, Guo S, Leneuve P, Dovero S, Diguet E, Tison F, Zhao B, Holzenberger M, Bezard E: IGF-1 signaling reduces neuroinflammatory response and sensitivity of neurons to MPTP. Neurobiol Aging 2009, 30:2021−2030
43. Fleissner F, Thum T: The IGF-1 receptor as a therapeutic target to improve endothelial progenitor cell function. Mol Med 2008, 14: 235−237
44. Imrie H, Viswambharan H, Sukumar P, Abbas A, Cubbon RM, Yuldasheva N, Gage M, Smith J, Galloway S, Skromna A, Rashid ST, Futers TS, Xuan S, Gatenby VK, Grant PJ, Channon KM, Beech DJ, Wheatcroft SB, Kearney MT: Novel role of the IGF-1 receptor in endothelial function and repair: studies in endothelium-targeted IGF-1 receptor transgenic mice. Diabetes 2012, 61: 2359−2368
45. Bäck K, Islam R, Johansson GS, Chisalita SI, Arnqvist HJ: Insulin and IGF1 receptors in human cardiac microvascular endothelial cells: metabolic, mitogenic and anti-inflammatory effects. J Endocrinol 2012, 215:89−96
46. Troncoso R, Ibarra C, Vicencio JM, Jaimovich E, Lavandero S: New insights into IGF-1 signaling in the heart. Trends Endocrinol Metab 2014, 25:128−137
47. Zhang L, Wang XH, Wang H, Du J, Mitch WE: Satellite cell dysfunction and impaired IGF-1 signaling cause CKD-induced muscle atrophy. J Am Soc Nephrol 2010, 21:419−427
48. Benedito R, Roca C, Sorensen I, Adams S, Gossler A, Fruttiger M, Adams RH: The notch ligands dll4 and jagged1 have opposing effects on angiogenesis. Cell 2009, 137:1124−1135

49. Wang Y, Liang A, Luo J, Liang M, Han G, Mitch WE, Cheng J: Blocking Notch in endothelial cells prevents arteriovenous fistula failure despite CKD. J Am Soc Nephrol 2014, 25:773–783
50. Kapitsinou PP, Sano H, Michael M, Kobayashi H, Davidoff O, Bian A, Yao B, Zhang MZ, Harris RC, Duffy KJ, Erickson-Miller CL, Sutton TA, Haase VH: Endothelial HIF-2 mediates protection and recovery from ischemic kidney injury. J Clin Invest 2014, 124:2396–2409
51. Dejana E, Giampietro C: Vascular endothelial-cadherin and vascular stability. Curr Opin Hematol 2012, 19:218–223
52. Vestweber D, Winderlich M, Cagna G, Nottebaum AF: Cell adhesion dynamics at endothelial junctions: VE-cadherin as a major player. Trends Cell Biol 2009, 19:8–15
53. Hao CN, Geng YJ, Li F, Yang T, Su DF, Duan JL, Li Y: Insulin-like growth factor-1 receptor activation prevents hydrogen peroxide-induced oxidative stress, mitochondrial dysfunction and apoptosis. Apoptosis 2011, 16:1118–1127
54. Canonici A, Steelant W, Rigot V, Khomitch-Baud A, Boutaghou-Cherid H, Bruyneel E, Van Roy F, Garrouste F, Pommier G, André F: Insulin-like growth factor-I receptor, E-cadherin and αv integrin form a dynamic complex under the control of α-catenin. Int J Cancer 2008, 122:572–582
55. Pennisi PA, Barr V, Nunez NP, Stannard B, Le Roith D: Reduced expression of insulin-like growth factor I receptors in MCF-7 breast cancer cells leads to a more metastatic phenotype. Cancer Res 2002, 62:6529–6537